Experimental Investigation of Pore Growth in Carbonaceous Nanoparticles During Low Temperature Oxidation by O_2

Tianyi Hu; Dr Chris Tighe

tianyi.hu16@imperial.ac.uk; c.tighe@imperial.ac.uk

Contents

1. **Introduction and motivation**

   Particulate matter (PM), diesel particulate filter (DPF), Printex U

2. **Research question and hypothesis**

   Internal burning, pore growth

3. **Methods**

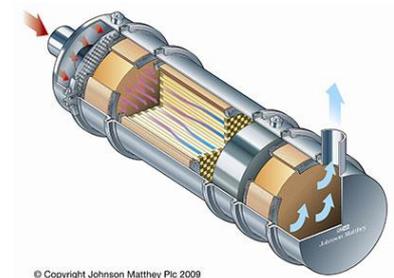   Transmission electron microscopy (TEM), thermogravimetric analyser (TGA), packed bed reactor

4. **Results and discussion**

   TGA mass transfer limitation, data deconvolution, random pore growth model, optimisation algorithm, activation energy
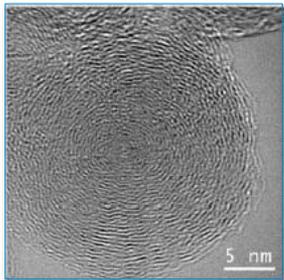
5. **Conclusions and future work**
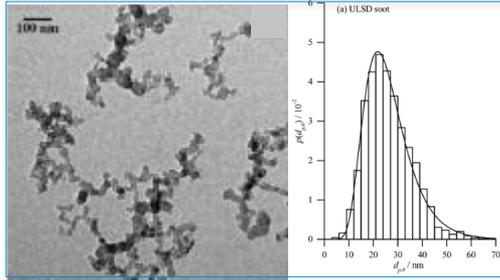
Imperial College London

Introduction

- Particulate matter (PM) emissions from diesel engines cause environmental pollution and harm to human health.

- Diesel particulate filters (DPF) remove these particulates from the exhaust.

- Emerging evidence that soot is oxidised on its exterior surface by NO_2 – external burning; while on the interior surface by O_2 – internal burning.

- Understanding the oxidation mechanism of soot particles in the filter is important for filter design and operation, and catalyst optimisation.

- The carbon black Printex U is often used as a surrogate soot for research purposes.

Motivation

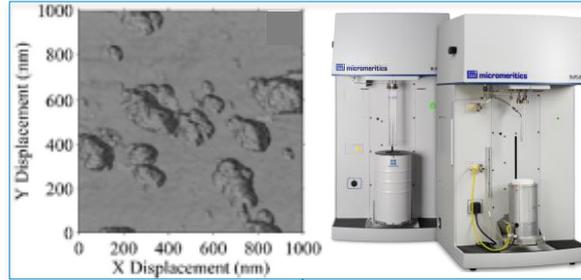| HRTEM		TEM		Packed bed, TGA and BET		DPF
- Single spherule	→	- An agglomerate	→	- An ensemble of agglomerates	→	- Thick layers of soot

(a) (b) (c) (d) (e) (f)

✓ well controlled experiments on a large ensemble of dispersed soot particles

(a) High Resolution TEM (HRTEM) image at 800k magnification of FT soot [1].

(b) TEM image of ULSD soot [2].

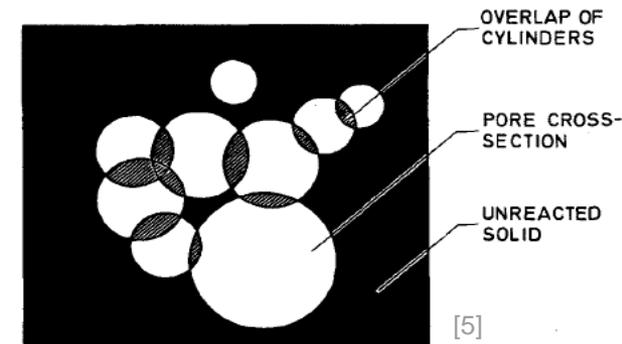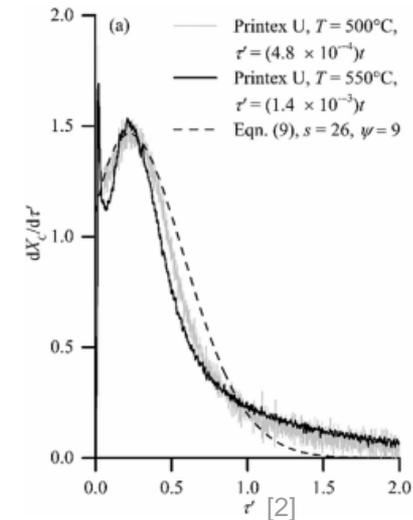(c) Distribution of diameters of ULSD soot spherules [2].

(d) Atomic force microscope (AFM) image of soot particles on the surface of a sand particle [2].

(e) Micromeritics 3Flex Surface Characterization Analyser [3].

(f) DPF before and after regeneration [4].

[1] J. Song et al. / Combustion and Flame 146 (2006) 589–604.
[2] C.J. Tighe et al. / Carbon 107 (2016) 20-35 .
[3] https://www.poretech.co.za/product/3-flex-surface-characterization-analyzer/
[4] https://goo.gl/images/K39Evb

Research Questions and Hypotheses

➢ What is the explanation for the second maximum in reaction rates of Printex U combusted in O_2?

- Burning inside spherules?

➢ How does the micro-structure of Printex U particles change during burnout?

- Pore growth and intersection within spherules [5]?

➢ Are oxidation experiments carried out using a thermogravimetric analyser (TGA) limited by mass transfer?

(a) Printex U, $T = 500°C$, $t' = (4.8 \times 10^{-4})t$
Printex U, $T = 550°C$, $t' = (1.4 \times 10^{-3})t$
Eqn. (9), $s = 26$, $\psi = 9$ [2]

OVERLAP OF CYLINDERS
PORE CROSS-SECTION
UNREACTED SOLID
[5]

[2] Tighe, C.J., Twigg, M.V., Hayhurst, A.N., Dennis, J.S. 2016. *Carbon*, 107, 20–35.
[5] Bhatia, S. K. & Perlmutter, D. D. 1980. AIChE Journal, 26, 379-386.

Method

	TGA	Packed Bed Reactor
Sample	Mixture of Printex U and quartz sand	
	50 mg (3.226 wt% Printex U)	2 g (0.008 wt% Printex U)
Apparatus	Simultaneous Thermal Analyser (STA)	Eurotherm 3508 and FTIR
Heat Treatment	Temperature ramp: 20 °C to 650 °C Heat-treatment: 650 °C for half an hour (where applicable, decrease to reaction temperature)	
	40 mL min^{-1} Ar	200 mL min^{-1} Ar
Reaction Temperature	650 °C	650 °C , 600 °C and 550 °C
Oxidation Experiment	Gas mixture of O_2 (11 vol%) and Ar	
	40 mL min^{-1}	200 mL min^{-1} (after reaction, product stream was diluted by 2 L min^{-1} Ar for FTIR analysis)

Imperial College London

Apparatus

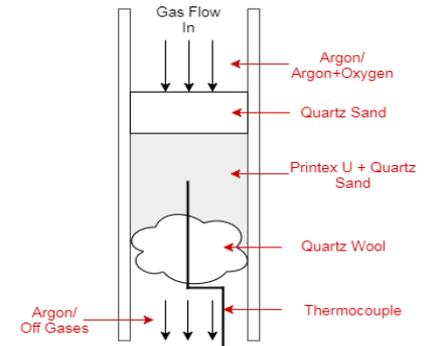- Packed bed reactor experiment

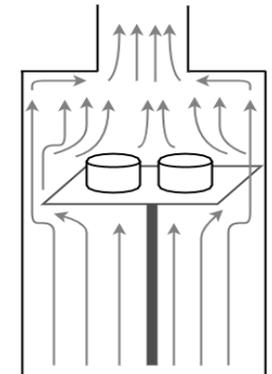FTIR

Temperature controller

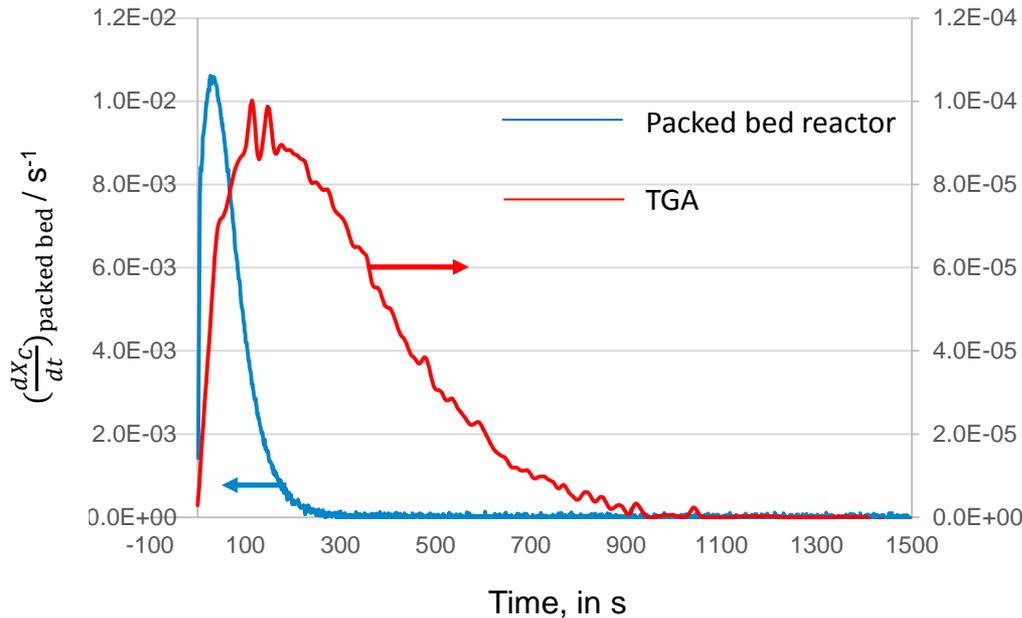Packed bed reactor

- TGA experiment

Netzch Jupiter STA

Simultaneous thermal analyser (STA)

- Thermogravimetry (TGA): weight changes
- Calorimetry (DSC): heat flows

Crucibles and gas flow

Results – TGA vs. Packed bed

	Packed Bed	TGA	Ratio
Reaction Time (s)	~300	~1000	~0.03
Maximum Rate (s⁻¹)	~1×10^{-2}	~1×10^{-4}	~100

- 650 °C, 11 vol% O_2

- $(\frac{dX}{dt})_{\text{TGA}}$: from direct measurement of mass

- $(\frac{dX_C}{dt})_{\text{packed bed}}$: from measurement of CO and CO_2 in off gases

- TGA:
  - longer reaction time;
  - lower reaction rate

- In this case, soot oxidation in TGA is controlled by the mass transfer, rather than the intrinsic reaction.

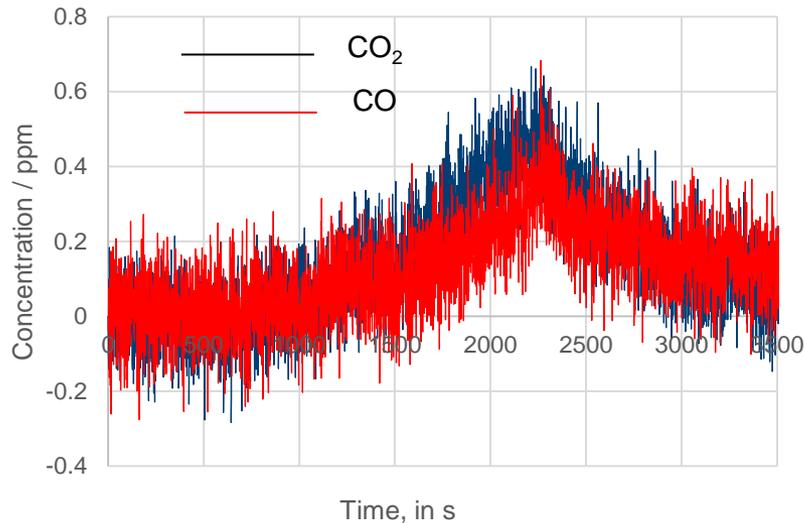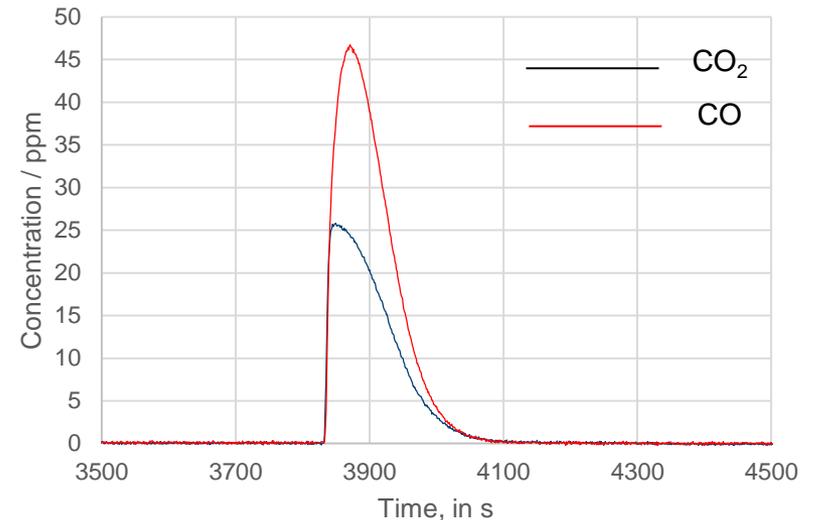- TGA experiments can be affected by several factors.

Results – Heat of Combustion

Combustion heat: -27411 mJ
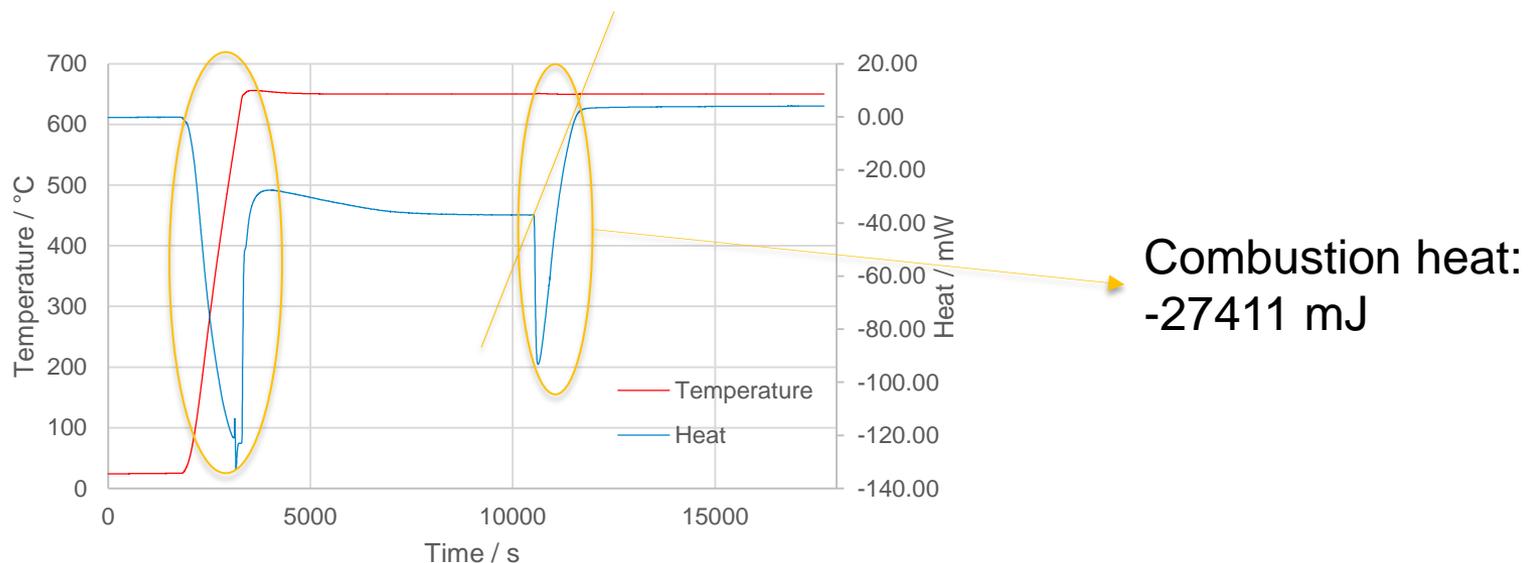
From measured combustion heat $\quad \Delta H_r(650°C) = -182.74$ kJ mol^{-1}

$$C + O_2 \rightarrow CO_2 \qquad\qquad \Delta H^0_{298K} = -394 \text{ kJ mol}^{-1}$$

$$C + \tfrac{1}{2} O_2 \rightarrow CO \qquad\qquad \Delta H^0_{298K} = -110 \text{ kJ mol}^{-1}$$

Results – Mass balance of C
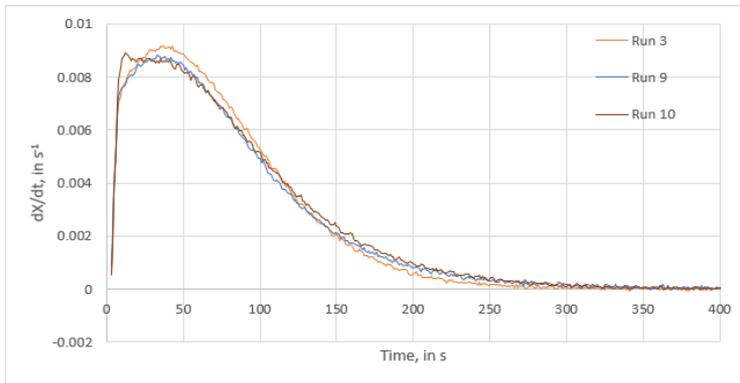

(a) Heat treatment period

(b) Reaction period

- More CO was produced than CO_2 during combustion.

- Concentration integration of CO and CO_2 gives the total carbon amount.

- Comparison of the calculated carbon mass with the weighed one gives discrepancies of 5~10%, which could result from tiny systematic errors in concentration measurements.
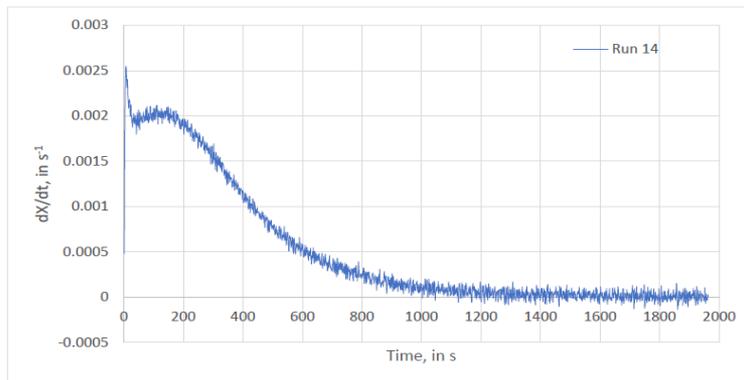
Results – Reaction rates
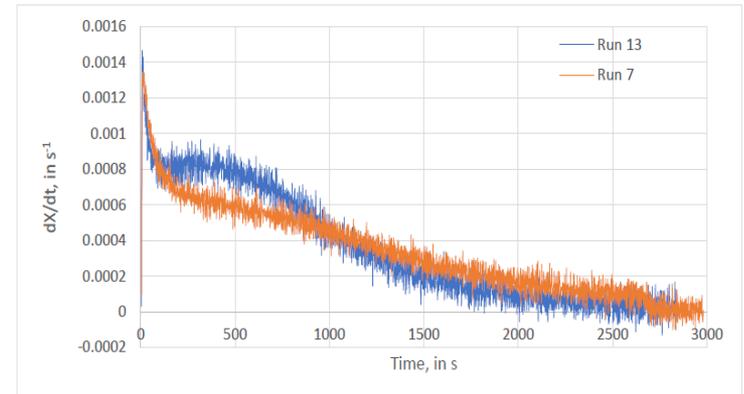
650 °C

- Packed bed reactor experimental results at three temperatures

- Deconvoluted FTIR measurements (in 200 mL gas cell, residence time ~ 6 s) to obtain concentration profiles from outlet of the packed bed

600 °C

550 °C

Results – Modelling

➢ Method:
- Fit the model to experimental data
- Optimise adjustable parameters f and $\varepsilon_{p,0}$
- Scrutinise fittings and parameter values.

$$\frac{dX_C}{d\tau'} = \left[\left(1 - \frac{\tau'}{s}\right)^3\left(1 + \frac{\psi\tau'}{2}\right) + \frac{3}{s}\left(1 - \frac{\tau'}{s}\right)^2\right]\exp\left[-\tau'\left(1 + \frac{\psi\tau'}{4}\right)\right] \quad (1)$$

Bhatia and Perlmutter's (1980) pore growth and intersection model [5].

$$\tau' = f \cdot t \quad (2)$$

$$f = \left(\frac{dX_C}{dt}\right)_{t=0} / \left(1 + \frac{3}{s}\right) \quad (3)$$

$$s = d_{p,0}S_{p,0}/2(1 - \varepsilon_{p,0}) \quad (4)$$

$$S_{p,0} = \rho_p(1 - \varepsilon_{p,0})S_{BET} \quad (5)$$

$$\psi = -1/\ln(1 - \varepsilon_{p,0}) \quad (6)$$

τ' – dimensionless time; t – time;

f – scaling factor;

$d_{p,0}$ – initial diameter of soot spherule;
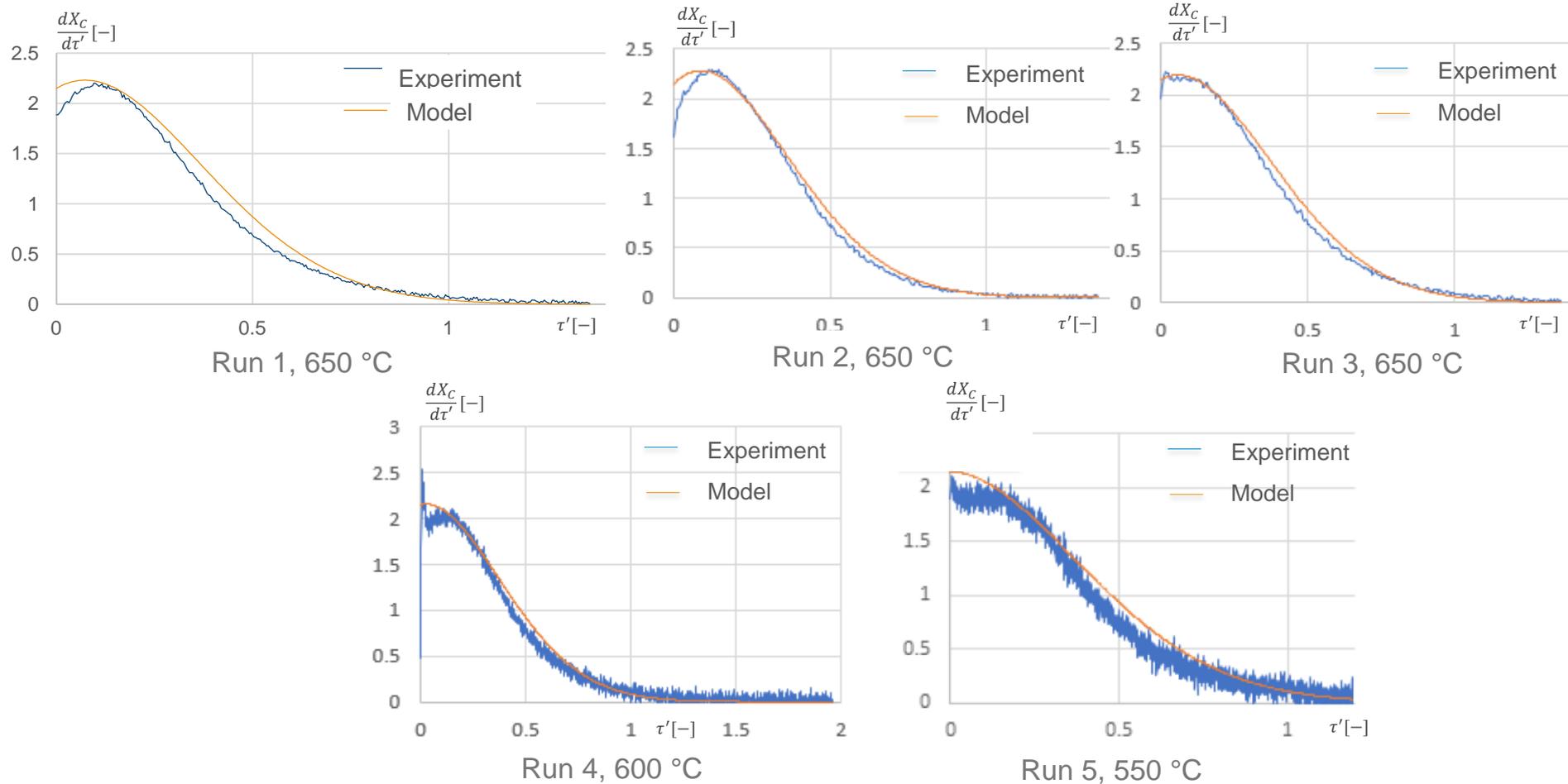$S_{p,0}$ – initial reacting surface area per unit volume;

ρ_p – skeletal density of carbon particle;
$\varepsilon_{p,0}$ – initial porosity;
S_{BET} – surface area measured by BET method;

ψ – dimensionless parameter representing uniform initial pore structure.

[5] Bhatia, S. K. & Perlmutter, D. D. 1980. AIChE Journal, 26, 379-386.

Results – Fitting

Run 1, 650 °C

Run 2, 650 °C

Run 3, 650 °C

Run 4, 600 °C

Run 5, 550 °C

Results – Minimisation results

Temperature	Run	f	$\varepsilon_{p,0}$	$\left(\dfrac{dX}{dt}\right)_{t=0}$	Deviation
650 °C	1	0.0040	0.08	0.0086 s^{-1}	**0.104**
	2	0.0040	0.07	0.0086 s^{-1}	**0.077**
	3	0.0040	0.09	0.0086 s^{-1}	**0.063**
600 °C	4	0.0010	0.11	0.0022 s^{-1}	**0.097**
550 °C	5	0.00047	0.19	0.0010 s^{-1}	**0.162**

- The fittings of reaction rate against time were better at higher temperatures.

- Repeatable parameter values were obtained at 650 °C.

- Initial rates and initial porosities were within a reasonable range for Printex U at corresponding reaction conditions.

Results – Activation energy

- In fact, f is related to the intrinsic rate of oxidation expressed by a rate equation e.g.

Rate constant based on surface area

Concentration of O_2, n is the reaction order

$$f = k_s C_{O_2}^n / [\rho_M (1 - \varepsilon_{p,0})]$$

Molar density of soot

- For pseudo-homogeneous burning, apparent activation energy E can be correlated with f by

$$\ln f = -\frac{E}{R} \cdot \frac{1}{T} + \ln A_f$$

Pre-exponential factor associated with f

$1/T$, in K^{-1}

$\ln f$

y = -16157x + 11.851
R² = 0.9599
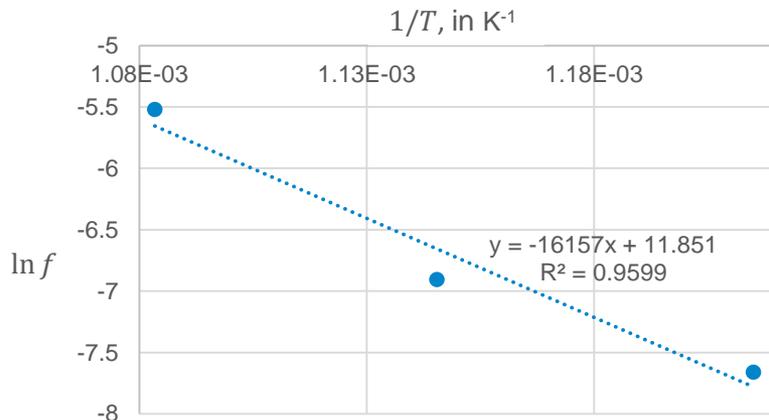
➤ E = 134.3 $\pm$ 27.5 kJ mol^{-1}

(cf. 145 $\pm$ 8 kJ mol^{-1} for ULSD soot and B90 soot, in the temperature range of 450 – 550 °C, at O$_2$ contents of 2.7 – 24.4 vol%.) [1]

➤ no diffusional limitation in this packed bed reactor system.

- strongly diffusion-limited: 8 – 24 kJ mol^{-1}

- reaction rate-limited: $\sim$200 kJ mol^{-1} [2]

[1] Tighe, C.J., Twigg, M.V., Hayhurst, A.N., Dennis, J.S. 2016. *Carbon*, 107, 20–35.
[2] Fogler, H.S. 2006. *Elements of chemical reaction engineering*, Upper Saddle River, NJ, Pearson Education Internat.

Next step – BET measurement

➢ Targets:
- total soot surface area as the reaction progresses (0 s, 5 s, 10s, etc);
- soot microporosity (0 s, 5 s, 10 s, etc).
- using dilute carbon/quartz mixtures from packed bed experiments

➢ Methods:
- Micromeritics 3Flex (to replace TriStar) for micropores
- Kr (to replace N_2): high sensitivity and accuracy for low surface areas

➢ Preliminary results

Imperial College London
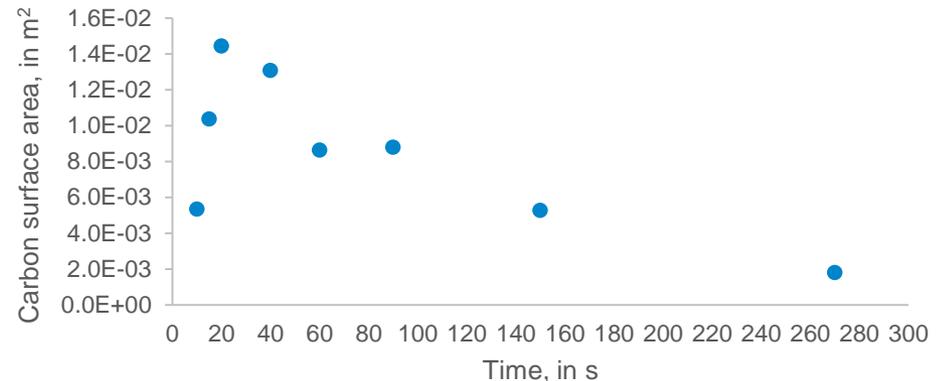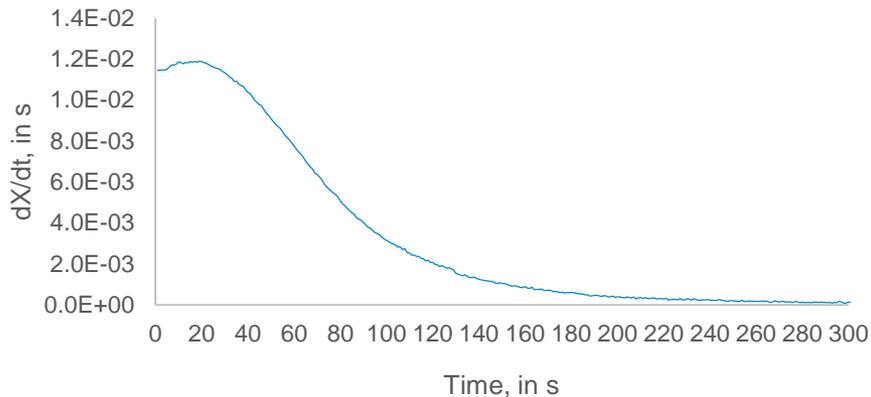
Conclusion

✓ The method developed in this research is suitable for studying the oxidation behavior of **an ensemble of soot agglomerates** under well controlled conditions.

✓ The results support the **pore evolution** of Printex U particles during oxidation by O_2 and suggest that internal burning occurs when the particles react with O_2.

✓ BET surface area and porosity measurements will provide direct evidence for the **internal burning** of the particles and assist the model fitting process.

✓ The method can be applied to investigate **diesel soot oxidation** under the conditions in a **DPF**. Findings of such studies will elucidate the modes and mechanisms of diesel soot oxidation and help the DPF design for an effective **reduction of PM emissions** from **diesel engines**.

Imperial College London

Acknowledgements

Dr Martyn Twigg, Prof Allan Hayhurst & Prof John Dennis for initiating this work

Mr Patrick Raffaelle and High Pressure Industrial Systems group

Imperial College London

Questions?

Imperial College London

Appendix – Sample preparation

- The sample is a mixture of Printex U and quartz sand (150 – 200 μm)
  - Printex U contents: - packed bed reactor experiments (0.008 wt%); - TGA experiments (3.226 wt%)

- TEM image of Printex U
  - Agglomerates of spherules: individual spherules of tens of nanometres in diameter

- Carbon content in Printex U: 91.3$\pm$0.4 wt%

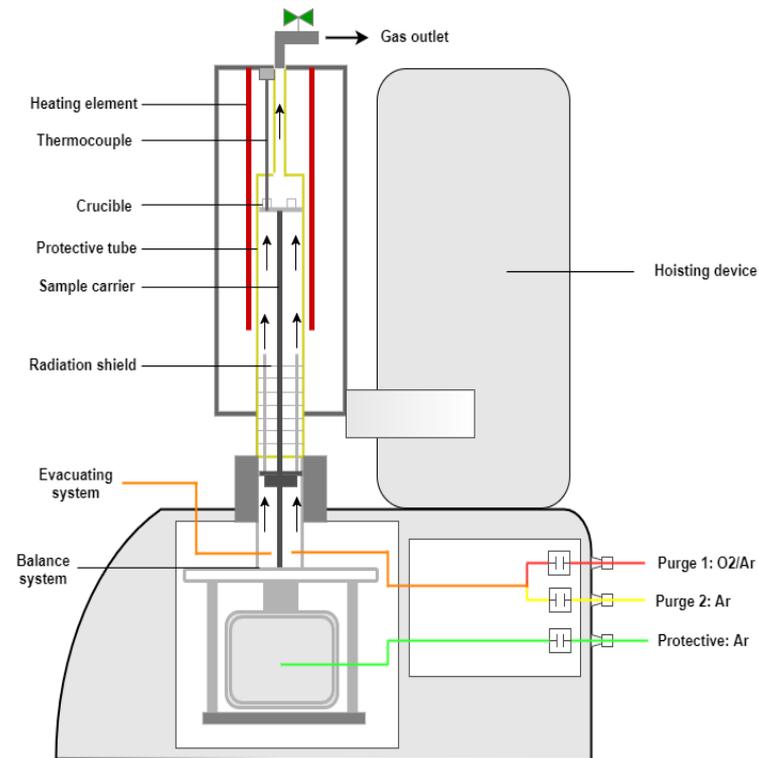- Surface area and pore size ($d_{pore} = 4V_{pore}/S_{pore}$)

200 nm

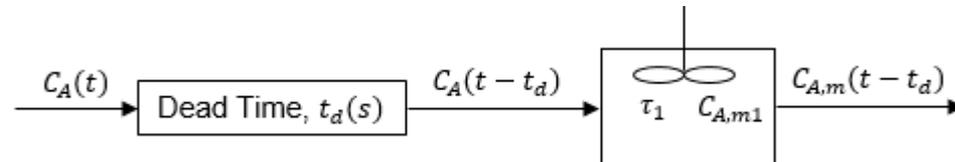| S_{BET} (m^{2}g^{-1})	S_{pore} (m^{2}g^{-1})	d_{pore} (nm)
82.8	77.1	14.3
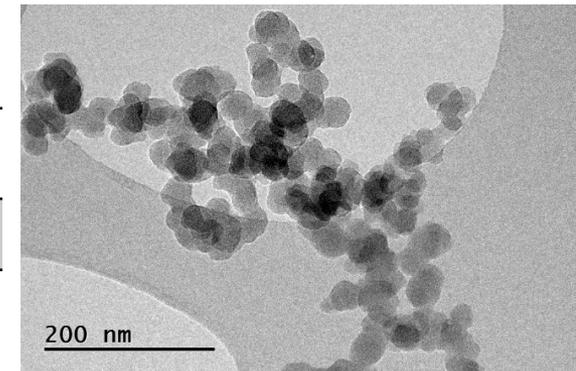
Appendix – Process flow diagram
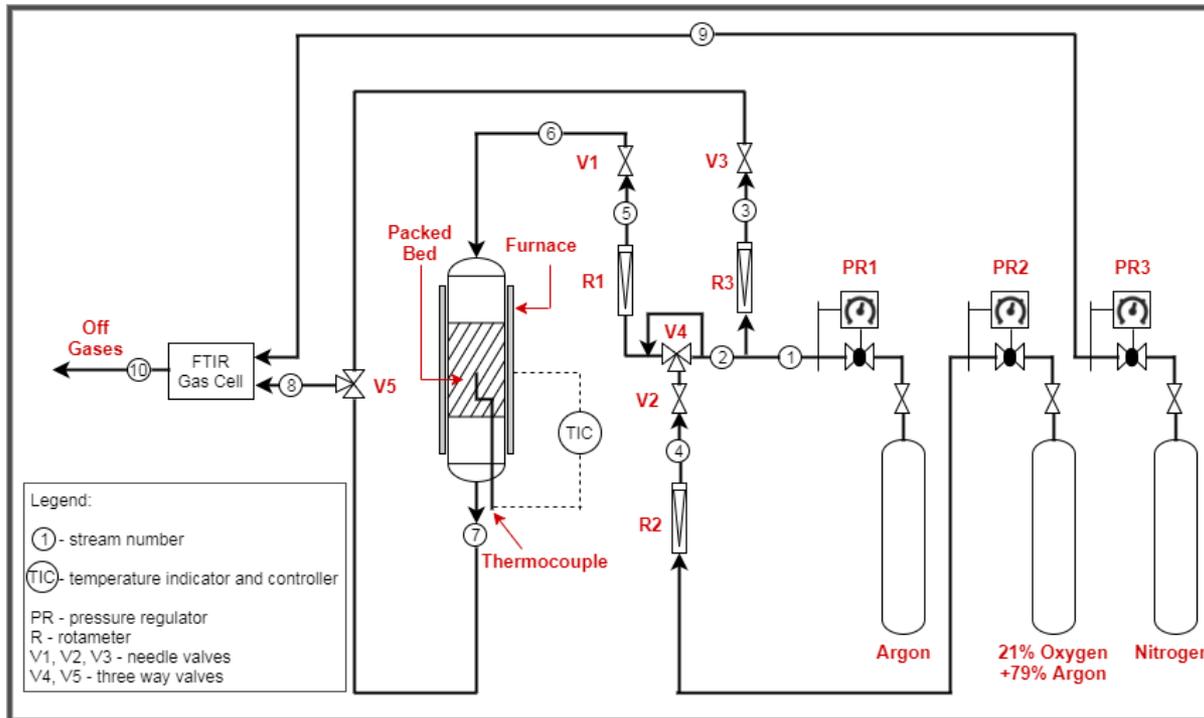
Appendix – STA

Appendix – Deconvolution (1)

➢ Model of a measurement system

$$C_A(t - t_d) = C_{A,m1} + \tau_1 \frac{dC_{A,m1}}{dt}$$

➢ Finite impulse response (FIR) filter

$$Y_i = \sum_{j=-m}^{n} X_{i-j} h_j$$

Y_i: deconvolved concentration measurement

X_{i-j}: raw measurement

h_j: FIR filter

X_{i-j}, Y_i and h_j: 1-D arrays of $1 \times k$, $1 \times (m+k+n)$ and $1 \times (m+k+n)$

m, k and n: (integers) number of elements;

i and j: (integer indices) the ith and the jth elements in the arrays

Appendix – Deconvolution (2)

$$h_{id} = \begin{matrix} j = -m & \dots & -1 & 0 & 1 & \dots & n \\ [0 & \dots & 0 & 1 & 0 & \dots & 0] \end{matrix}$$

$$h_{sdiff} = \begin{matrix} j = -2 & -1 & 0 & 1 & 2 \\ [0.2/\Delta t & 0.1/\Delta t & 0 & -0.2/\Delta t & -0.1/\Delta t] \end{matrix}$$
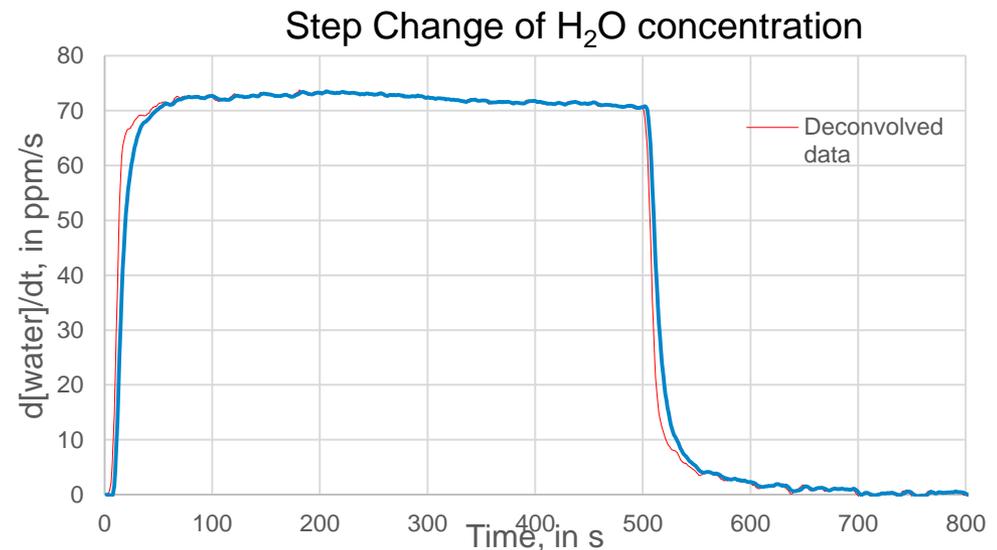
$$h_{ms} = h_{id} + \tau_1 h_{sdiff}$$

$$= \begin{matrix} j = -2 & -1 & 0 & 1 & 2 \\ [0.2\tau_1 & 0.1\tau_1 & 0 & -0.2\tau_1 & -0.1\tau_1] \end{matrix}$$

$$\tau_1 = \frac{V}{Q} = \frac{0.2\ L}{2.26\ L/min} = 0.09\ min = 5.31\ s$$

$$h_{ms} = [1.06 \quad 0.53 \quad 0 \quad -1.06 \quad -0.53]$$

- Identity filter: generating an identical array

- Smoothing filter: reducing noise

Step Change of H_2O concentration

Deconvolved data

d[water]/dt, in ppm/s — Time, in s
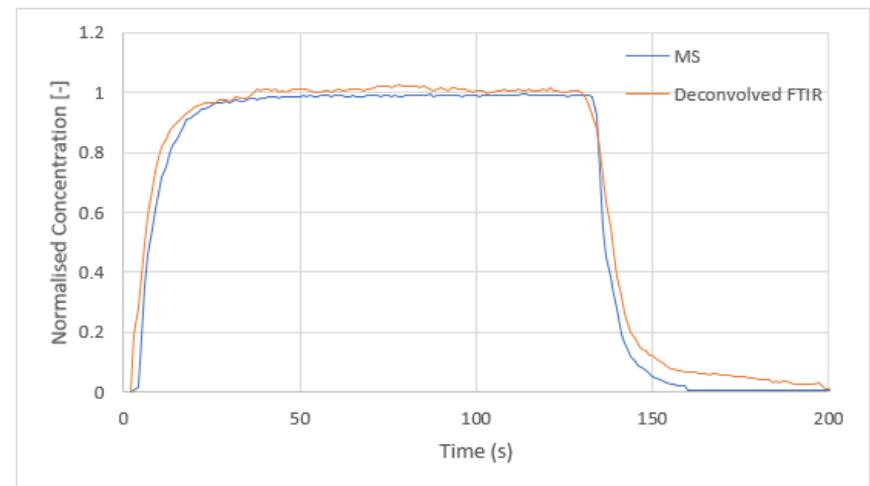
Appendix – Mass spectrometer

- Sample flowrate: 10 mL min^{-1}

- Fast response

- FTIR flowrate = 895 mL min^{-1}
  Theoretical τ_1 = 13.41 s
  Optimised τ_1 = 7.92 s

➢ FTIR gas cell: not likely to have perfect mixing

➢ Use MS to obtain residence time distribution in a FTIR gas cell for certain gas flowrates

Raw measurement MS vs. FTIR
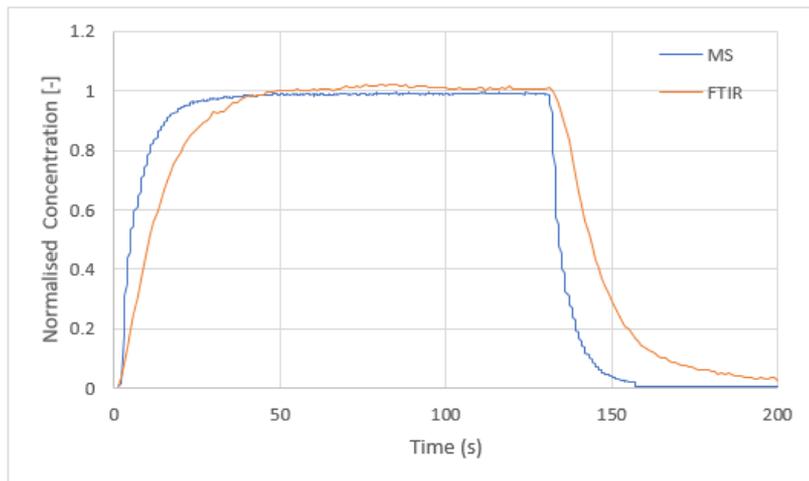
MS vs. FTIR (Deconvolved)

Appendix – Optimisation

Changes of Deviation with $\varepsilon_{p,0}$ and f

$\varepsilon_{p,0} \downarrow, f \rightarrow$	0.002	0.003	0.004	0.005	0.006
0.06	331.40	29.86	5.43	22.20	40.93
0.07	349.86	36.03	4.06	17.18	34.33
0.08	363.98	41.53	3.68	13.80	29.57
0.09	375.02	46.38	3.83	11.45	26.01
0.10	383.82	50.65	4.26	9.78	23.28

Appendix – BET

(1) Why Kr is more accurate than N2?

At 77K, vapour pressure of Kr is 2 mmHg, much smaller than N2 (760 mmHg). Thus, a small amount of pressure difference, i.e. low surface area can be accurately measured with Kr. That is to say, Kr is more sensitive to small pressure change. For the same reason, Xe is even better but more expensive.

(2) Pore limit

Table 7.1 Molecular Areas of Some Adsorptives

Adsorptive	T (K)	Cross-Sectional Area σ (nm^2)		
		Literature Range[a]	In Close-Packed Liquid Monolayer[b]	Customary Value
Nitrogen	77	0.13–0.20	0.162	0.162
Argon	77	0.10–0.19	0.138	0.138
Krypton	77	0.14–0.24	0.152	0.202
Xenon	77	0.16–0.25	0.168[c]	0.170
Oxygen	77	0.13–0.20	0.141	0.141
Carbon dioxide	195	0.14–0.22	0.163	0.210

[6]

[6] Rouquerol, F.i., Adsorption by powders and porous solids : principles, methodology and applications. 2nd ed. 2013, Oxford: Academic Press.